communications biology

A Nature Portfolio journal

Article

https://doi.org/10.1038/s42003-025-08119-3

IL-33/ST2 drives inflammatory pain via CCL2 signaling and activation of TRPV1 and TRPM8

Linjie Wang[1,9], Jingyun Zhang[1,2,9], Shijuan Qiu[1,9], Ruizhen Huang[1], Yuge Wang[1], Yuting Wang[1], Mingyu Li[1], Qingqing Ye[3], Sibo Zhang[4], Zhenhua Qi[3], Lan Cao[1], Guohao Li[5,6], Yajie An[1], Denghui Xie[5,6], Wenli Mi[7], Huaqiao Wang[1], Tao Luo[1], Jingdun Xie[3] & Junting Huang[1,8]

Innate immunity is the first line of host defense and contributes to pain. However, how innate immune system interacts with sensory neurons to govern pain remains poorly understood. Here, we report that interleukin 33(IL-33) initiates pain hypersensitivity that requires chemokine (C-C motif) ligand 2 (CCL2) secretion from infiltrated macrophages and neutrophils and activation of transient receptor potential vanilloid 1 (TRPV1) and transient receptor potential melastatin 8 (TRPM8) channels in sensory neurons. Blocking CCL2 receptor (CCR2) attenuates IL-33- induced and Complete Freund's adjuvant (CFA)-induced thermal hyperalgesia and blocking TRPV1 and TRPM8 attenuates IL-33-induced mechanical and thermal hypersensitivity and cold allodynia respectively. Furthermore, depletion of macrophages reduces IL-33-induced pain and expression of *CCL2* and suppression of tumorigenicity 2 (*ST2*) in hindpaw skin and inhibition of CCR2 prevents recruitment of macrophages and neutrophils. Our findings reveal an unrecognized neuroimmune crosstalk of IL-33-CCL2 signaling from infiltrated immune cells with TRPV1/TRPM8 in sensory neurons to facilitate pain states.

Pathogens cause inflammation and pain, and the host defense plays a critical role in this process. Acute pain resolves with resolution of inflammation, whereas it turns to chronic states as the inflammation consistently exists[1,2]. Specifically, activation of innate immunity triggers pain via pattern recognition receptors such as toll-like receptors (TLRs)[3–5] and inflammasomes[6,7]. However, the underlying mechanisms on how innate immune system interacts with sensory neurons to drive pain remains poorly understood.

IL-33 is an alarmin cytokine that was first discovered in human endothelial cells[8] and was identified as the ligand for ST2 receptor[9]. The IL-33 locates in nuclei for regulating gene expression under physiological state and is massively released during pathogenic infection, allergen exposure or tissue injury[10]. The IL-33-ST2 signaling plays a crucial role in immune system via activation of immune cells such as Group 2 innate lymphoid cells (ILC2s), Th2, Treg and CD8 + T cells[11]. IL-33 has also been reported to function in the central nervous system and neurological diseases[12–15]. Interestingly, IL-33 is protective in the Alzheimer's disease[16,17] and stroke[18,19], whereas it facilitates pain hypersensitivity[20–22]. Intraplantar or intraarticular injection of IL-33 induces nociception[23] and the IL-33-ST2 signaling implicates in various pain models such as formalin[24,25], carrageenin[26], gout arthritis[27], osteoarthritis[28] and CFA-induced[29] inflammatory models; and the spared nerve injury (SNI)[30], chronic constriction injury (CCI)[31,32] and infraorbital nerve injury (IONI) -induced neuropathic models[33]. We previously showed that hyperactivity of innate immunity triggers pain via activation of TLR2-NLRP3-IL-33 signaling[34,35]. However, how IL-33 activates innate immunity and interacts with sensory neurons to promote pain states is still elusive.

The CCL2, known as monocyte chemoattractant protein-1 (MCP-1), is a chemotactic mediator that recruits monocytes to the injury site[36]. CCL2

[1]Department of Human Anatomy and Physiology, Zhongshan School of Medicine, Sun Yat-Sen University, Guangzhou, China. [2]Central Laboratory, The Third Affiliated Hospital of Sun Yat-sen University, Guangzhou, China. [3]Department of Anesthesiology, State Key Laboratory of Oncology in South China, Guangdong Provincial Clinical Research Center for Cancer, Sun Yat-sen University Cancer Center, Guangzhou, China. [4]Foshan Clinical Medical School, Guangzhou University of Chinese Medicine, Foshan, China. [5]Department of Joint Surgery and Sports Medicine, Center for Orthopedic Surgery, Orthopedic Hospital of Guangdong Province, The Third Affiliated Hospital of Southern Medical University, Guangzhou, China. [6]Guangdong Provincial Key Laboratory of Bone and Joint Degeneration Diseases, Academy of Orthopedics, Guangzhou, China. [7]Department of Integrative Medicine and Neurobiology, School of Basic Medical Sciences, Shanghai Medical College, Institutes of Integrative Medicine, Fudan University, Shanghai, China. [8]Guangdong Province Key Laboratory of Brain Function and Disease, Zhongshan Medical School, Sun Yat-sen University, Guangzhou, China. [9]These authors contributed equally: Linjie Wang, Jingyun Zhang, Shijuan Qiu.
e-mail: Huangjt56@mail.sysu.edu.cn

was up-regulated in dorsal root ganglion (DRG) neurons in neuropathic pain and intrathecal injection of CCL2 induced mechanical hypersensitivity[37]. A line of evidence further shows that CCL2 modulates pain hypersensitivity via sensitization of TRPV1 and Nav1.8 channels in DRG neurons[38,39], increase of spinal central sensitization[40], disturbing the excitatory/inhibitory synaptic balance[41] and enhancement of NMDA receptor-induced synaptic plasticity[42].

Here, we report that IL-33 initiates hyperactivity of innate immunity to release CCL2 that results in pain hypersensitivity via interaction of the infiltrated neutrophils and macrophages with TRPV1-positive and TRPM8-positive sensory neurons, revealing an un-recognized neuroimmune crosstalk to promote pain development.

Results

IL-33/ST2 activation triggers acute pain

We firstly examined whether IL-33 application induces acute pain. Intraplantar injection of IL-33 (200 ng/20 μL) decreased both paw withdrawal thresholds (Fig. 1A, C) and latencies (Fig. 1B, D) at 4 h in male and female mice. Similarly, IL-33 induces cold allodynia in both male (Fig. 1E) and female mice (Fig. 1F). We then determined whether blocking ST2 reverses IL-33-induced pain. ST2 neutralizing antibody was intraplantarly injected into the left hindpaw 30 min before IL-33 injection and then pain responses were tested at 1, 2, and 4 h after IL-33 application (Fig. 1G). As expected, pretreatment with ST2 neutralizing antibody (1 μg/10 μL) partially attenuated IL-33-induced mechanical allodynia (Fig. 1H) and thermal hyperalgesia (Fig. 1I) at 1 and 2 h after IL-33 injection. The ST2-null (*ST2*−/−, Supplementary Fig. S1A) and IL-33-null (*IL-33*−/−, Supplementary Fig. S1B) mice were genotyped by PCR gels. In *ST2*−/− mice, IL-33-induced mechanical (Fig. 1J, L) and thermal hypersensitivity (Fig. 1K, M) were respectively reversed in male and female of *ST2*−/− mice. Overall, these data indicate that IL-33/ST2 activation elicits acute pain.

IL-33/ST2 maintains chronic inflammatory pain

Given that IL-33/ST2 activation induces acute pain, we further examined their functions in chronic inflammatory pain. As expected, mechanical allodynia (Fig. 2A) and thermal hyperalgesia (Fig. 2B) was partially reversed in both *IL-33*−/− and *ST2*−/− male mice at day 3 after CFA injection and similar effects were observed at day 9 (Fig. 2C–D). We also tested these effects in female mice. As shown, CFA-induced mechanical allodynia and thermal hyperalgesia were attenuated in the ipsilateral (Fig. 2E–F) but not the contralateral hindpaw (Supplementary Fig. S1C, D) in *IL-33*−/− female mice. Similarly, both mechanical allodynia (Fig. 2G and Fig. 2I) and thermal hyperalgesia (Fig. 2H, J) were also attenuated in *ST2*−/− female at day 3 and day 9 after CFA injection, while the thermal hyperalgesia was not altered in the contralateral hindpaw (Supplementary Fig. S1E) in *ST2*−/− female mice. We extended the findings to the mono-iodoacetate (MIA)-induced osteoarthritic pain model. As shown, the thermal hyperalgesia was also attenuated in *ST2*−/− male mice (Fig. 2K). Altogether, these data suggest that IL-33/ST2 signaling is essential for chronic pain in both male and female mice. We therefore used male mice in the following experiments.

IL-33 initiates pain hypersensitivity via upregulation of CCL2

We previously identified that TLR2 activation induces pain responses via IL-33, however, some interesting phenomena are still not clarified. For example, IL-33 does not initiate neuronal firing in DRGs in naïve mice but in pain-primed mice. This indicates a third component may play a critical role in IL-33-induced pain. As IL-33 activates ILC2s, we firstly detected mRNA levels of *IL-4, IL-9* and *IL-13* in the hindpaw and spinal cord at 4 h after intraplanar injection of IL-33. The gene expression of *IL-4, IL-9* and *IL-13* was neither altered in the hindpaw (Supplementary Fig. S2A–C) nor in the spinal cord (Supplementary Fig. S2D–F) after IL-33 injection, indicating ILC2s may not play an essential role in IL-33-triggered pain. We previously demonstrated that IL-33 and multiple other mediators were up-regulated in FSL1-induced pain[34]. We therefore examined some other inflammatory mediators such as *CCL2, CXCL1, CCL12* and *IL-17* that were up-regulated in FSL1-induced model. As shown, the mRNA levels of *CCL2* (Fig. 3A) and *CXCL1* (Fig. 3B) were up-regulated in the hindpaw at 4 h after IL-33 induction, whereas the mRNA levels of *CCL12* (Supplementary Fig. S2G) and *IL-17* (Supplementary Fig. S2H) were unaltered. We further examined their expression in spinal cord. Interestingly, gene expression of *CCL2* (Fig. 3C) but not *CXCL1* (Fig. 3D), *CCL12* (Supplementary Fig. S2I) and *IL-17* (Supplementary Fig. S2J) was increased in spinal cord at 4 h after IL-33 injection. As only *CCL2* was up-regulated in both hindpaw and spinal cord, we next examined the protein level of CCL2 in both hindpaw and spinal cord in the IL-33 model. The protein level of CCL2 was increased in hindpaw (Fig. 3E, F) but not in spinal cord (Fig. 3G, H). This discrepancy for gene and protein expression of CCL2 in spinal cord may be due to multiple factors such as mRNA translation rates, translation rate modulation, modulation of a protein's half-life, protein synthesis delay and protein transport[43]. The gene expression of *IL1β* was also up-regulated in the hindpaw after IL-33 injection (Fig. 3I). In addition, we measured serum levels of IL-33 in blood after intraplantar injection of PBS or IL-33. The protein levels of IL-33 are 2.17 ± 0.410(pg/mL) and 2.18 ± 0.398(pg/mL) in PBS-treated mice (n = 6 mice) and IL-33-treated mice (n = 7 mice) respectively, which is quite low concentration and is difficult for ELISA detection. This suggests that local injection of IL-33 may not induce systemic inflammation. Together, these data demonstrate CCL2 is the down-stream signal for IL-33-induced pain.

CCL2/CCR2 is required for IL-33-induced and CFA-induced inflammatory pain

Having established CCL2 as critical down-stream signal for IL-33, we then examined whether blocking CCL2/CCR2 regulates IL-33-induced or CFA-induced inflammatory pain. Intraplantar pretreatment with the CCR2 antagonist (INCB3344) does not alter mechanical (Fig. 4A) but attenuate IL-33-induced thermal hypersensitivity (Fig. 4B). Though the protein level of CCR2 (Supplementary Fig. S3A, B) does not change in the IL-33 model, blocking CCR2 with INCB3344 decreased gene expression of *CCL2* (Fig. 4C) and mRNA level of *CCL2* was reversed in *ST2*−/− mice (Fig. 4D) in the IL-33 model. We then examined the analgesic effects of INCB3344 in the CFA model. Similarly, INCB3344 administration does not affect the mechanical allodynia (Fig. 4E) but attenuates the thermal hyperalgesia (Fig. 4F) at day 3 after CFA injection. We further detected expression of CCL2 in the hindpaw skin from the *IL33*−/− and *ST2*−/− mice in the CFA model. Though the gene expression of *CCL2* was not altered in the hindpaw in *IL33*−/− mice (Supplementary Fig. S3C), the protein level of CCL2 was reversed in *ST2*−/− mice (Fig. 4G, H) at day 3 after CFA injection. These data indicate CCL2/CCR2 signals were required for IL-33 and CFA-induced thermal hyperalgesia. We further extended those findings to clinical patients with osteoarthritis(OA), which is characterized by pain. We took synovia and cartilages from osteoarthritic patients and patients with meniscus injury or injury of anterior cruciate ligament as non-OA control. As shown, gene expression of *CCL2* is significant higher (Fig. 4I) and there is an increased trend for gene expression of *IL-33* (Fig. 4J) in the synovia of OA patients. Furthermore, there was a positive correlation between gene expression of *IL-33* and *CCL2* in the synovia of OA patients (Fig. 4K) but not in non-OA patients (Supplementary Fig. S3D). There is an increase trend for gene expression of *ST2* in the synovia OA patients (Supplementary Fig. S3E) but no correlation between gene expression of *CCL2* and *ST2* (Supplementary Fig. S3F) in the synovia of OA patients. In addition, neither the gene expression of *IL-33* (Supplementary Fig. S3G) nor *CCL2* (Supplementary Fig. S3H) was changed between synovia and cartilage and no correlation was found for gene expression of *CCL2* and *IL-33* in cartilage (Supplementary Fig. S3F) in OA patients. These data further support the positive correlation between IL-33 and CCL2 in clinical OA pain.

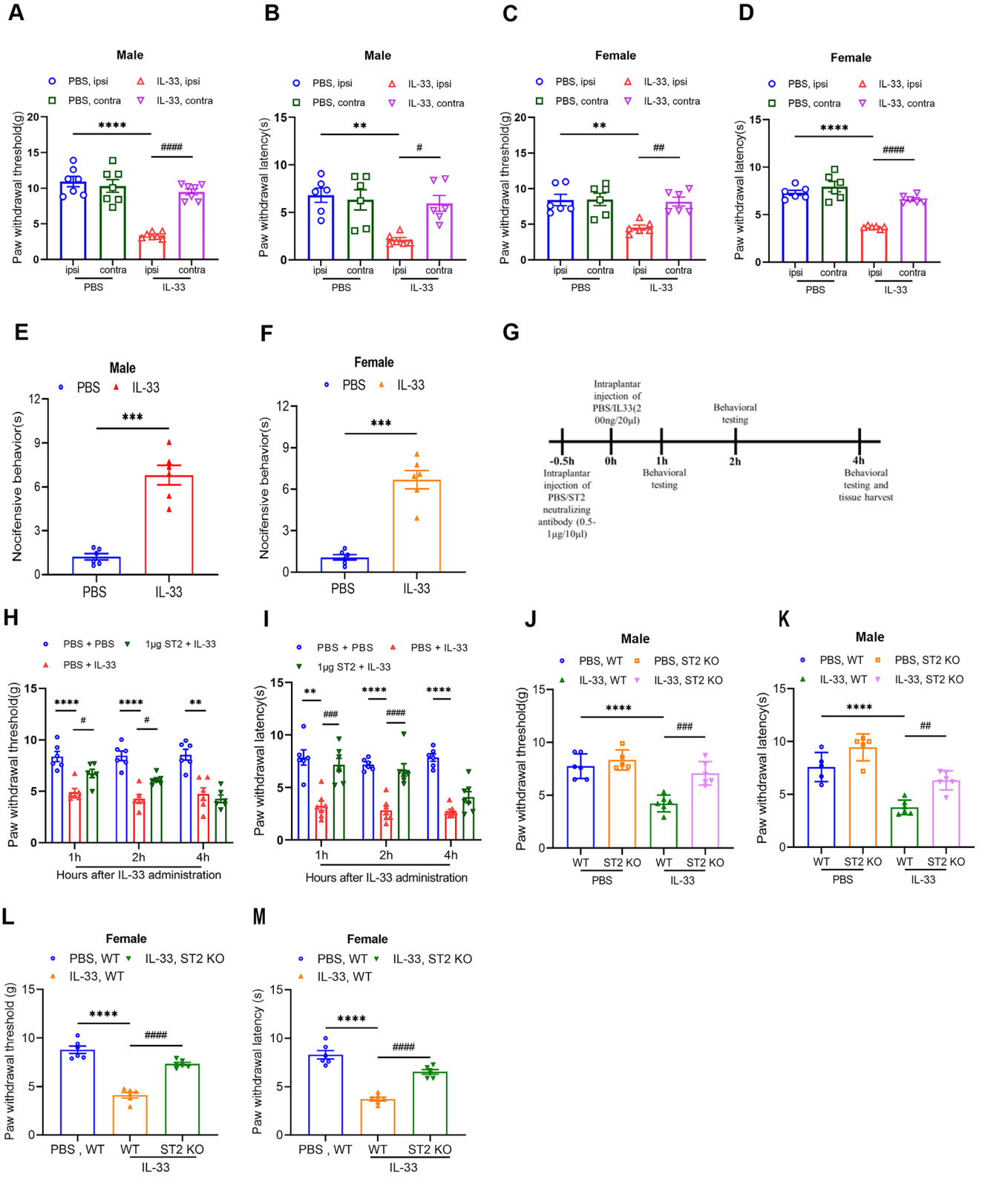

Fig. 1 | IL-33 triggers acute pain and blocking ST2 receptors relieves IL-33-induced pain. Intraplantar injection of IL-33(200 ng/20 μL) induces mechanical allodynia (**A**) and thermal hyperalgesia (**B**) in male mice (n = 6–7 mice). Intraplantar injection of IL-33(200 ng/20 μL) induces mechanical allodynia (**C**) and thermal hyperalgesia (**D**) in female mice (n = 6 mice). IL-33 induces cold allodynia in both male (**E**) and female (**F**) (n = 6 mice). **G** Schematic diagram shows the pre-treatment of ST2 neutralizing antibody in IL-33-induced pain model. **H**–**I** Pre-treatment of ST2 neutralizing antibody partially attenuates IL-33-induced thermal hyperalgesia (**F**) and mechanical allodynia (**G**) (n = 6-7 mice). **J**–**K** IL-33-induced paw withdrawal threshold (**H**) and paw withdrawal latency (**I**) were reversed in *ST2−/−* male mice (n = 5-6 mice). **L**–**M** IL-33-induced paw withdrawal threshold (**H**) and paw withdrawal latency (**I**) were reversed in *ST2−/−* female mice (n = 6 mice). Data are presented as mean ± SEM. $^{**}p < 0.01$, $^{***}p < 0.001$, $^{****}p < 0.0001$, $^{\#}p < 0.05$, $^{\#\#}p < 0.01$, $^{\#\#\#}p < 0.001$, $^{\#\#\#\#}p < 0.0001$. *represents PBS vs IL-33 in WT mice, #represents ipsi vs contra or WT vs *ST2−/−* in the IL-33 model. One-way ANOVA with Bonferroni's post hoc test for (**A**–**D**, **J**–**M**); Unpaired t-test for (**E**, **F**); Repeated measures for Two-way ANOVA with Bonferroni's post-hoc test for (**H**, **I**); ipsi ipsilateral, contr contralateral.

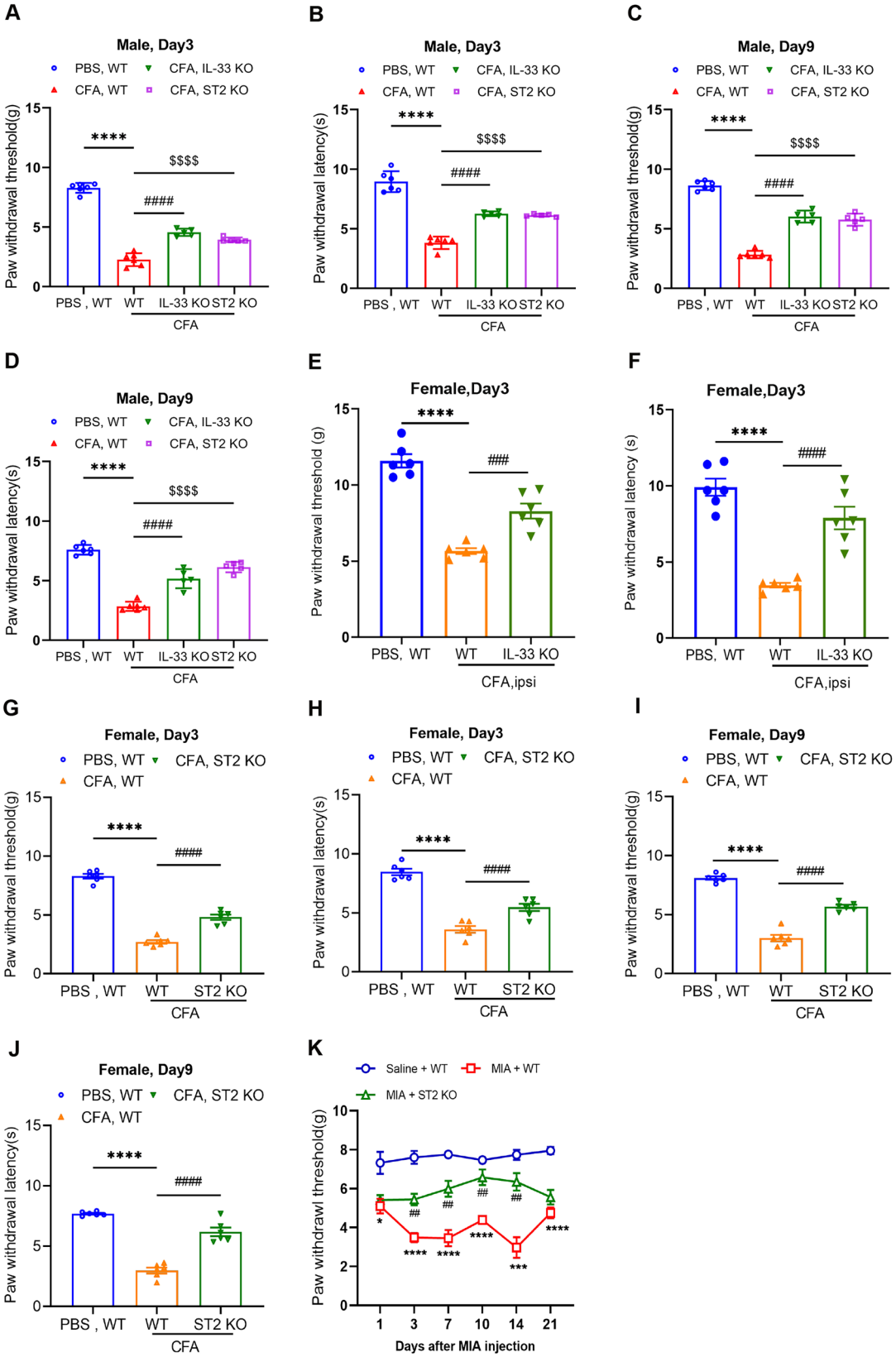

CCL2 is secreted by macrophages and neutrophils after IL-33 stimulation

Our next question is where does the CCL2 secrete from? Neutrophils and macrophages are the first batch of immune cells recruited to the injury site, we therefore co-stained CCL2 with neutrophil marker (Myeloperoxidase, MPO) and macrophage marker (F4/80). The number of neutrophils was increased in the hindpaw skin of IL33-treated mice (Fig. 5A, B) and the percentage of neutrophils that express CCL2 was elevated from 17.41% in PBS-treated mice to 33.80% in IL-33 treated mice (Fig. 5C) at 4 h after IL-33 injection. Similarly, infiltration of macrophages and the percentage of

Fig. 2 | IL-33/ST2 is required for chronic pain in both male and female mice in the CFA model. Mechanical allodynia (**A**) and thermal hyperalgesia (**B**) were attenuated in both *IL33−/−* and *ST2−/−* male mice at day 3 after CFA injection (n = 6 mice). Mechanical allodynia (**C**) and thermal hyperalgesia (**D**) were attenuated in both *IL33−/−* and *ST2−/−* male mice at day 9 after CFA injection (n = 6 mice). Mechanical allodynia (**E**) and thermal hyperalgesia (**F**) were partially reversed in the ipsilateral hindpaw of *IL-33−/−* female mice at day 3 after CFA injection (n = 6 mice). Mechanical allodynia (**G**) and thermal hyperalgesia (**H**) were partially reversed in the ipsilateral hindpaw of *ST2−/−* female mice at day 3 after CFA injection (n = 6 mice). Mechanical allodynia (**I**) and thermal hyperalgesia (**J**) were partially reversed in ST2−/− female mice at day 9 after CFA injection (n = 6 mice). **K** Mechanical allodynia was partially attenuated in *ST2−/−* male mice in the MIA model (n = 6 mice). Data are presented as mean ± SEM. $^{**}p < 0.01$, $^{****}p < 0.0001$, $^{\#}p < 0.05$, $^{\#\#\#}p < 0.001$, $^{\#\#\#\#}p < 0.0001$, $p < 0.0001$. *represents PBS vs CFA or MIA in WT mice. $^{\#}$represents WT vs *IL-33−/−* mice in (**A**–**F**) or *ST2−/−* in (**G**–**J**) for the CFA model and (**K**) in the MIA model, represents WT vs *ST2−/−* mice in the CFA model in (**A**–**D**). One-way ANOVA with Bonferroni's post-hoc test for (**A**–**J**); Repeated measures for Two-way ANOVA with Bonferroni's post-hoc test for (**K**); CFA complete Freund's adjuvant, MIA mono-iodoacetate.

macrophages that express CCL2 were increased in the IL33-treated mice (Fig. 5D–F, from 29.54% to 48.65%). We also quantified CCL2-positive number in area unit (co-staining with macrophages in Fig. 5D) and it was increased in the IL-33-treated mice (Supplementary Fig. S4A) which is consistent with the findings in Fig. 3A, F. In addition, we examined whether CCL2 was secreted from other cells in the hindpaw skin. Co-staining of CCL2 with the keratinocyte marker (K14) shows that they express in different layers of skin with no co-localization (Supplementary Fig. S4B). CCL2 expresses in a bunch of mast cells (tryptase as cell marker, Supplementary Fig. S4C) but rarely expresses in skin nerves (Supplementary Fig. S4D). These findings suggest that neutrophils, macrophages and mast cells could be the main sources for CCL2 secretion, and we focused on macrophages and neutrophils as they are the first batch to reach the injury sites. To further confirm this, we intraperitoneally injected clodronate liposome (i.p: 200 μL) once a day for two days to ablate macrophages. As shown, depletion of macrophages attenuated IL-33-induced mechanical (Fig. 5G) and thermal hypersensitivity (Fig. 5H) and reversed the up-regulation of *CCL2* (Fig. 5I) and *ST2* (Fig. 5J). In the CFA model, we also observed the increase of ST2 (Supplementary Fig. S4E, F), infiltration of macrophages (Supplementary Fig. S4G) and percentage of ST2-expressing macrophages (Supplementary Fig. S4H). In addition, in vitro stimulation of Raw264.7 (cell-line of macrophages) with IL-33 for 24 h dramatically increased the secretion of CCL2 from 65.4 pg/ml in PBS group to 803.8 pg/ml in IL-33-treated (50 ng/mL) group (Fig. 5O). Together, these findings suggest that secretion of CCL2 from neutrophils and macrophages is IL-33-dependent.

We further examined whether blocking CCR2 affects infiltration of macrophages and neutrophils. Interestingly, infiltration of F4/80-positive macrophages (Fig. 5L) and MPO-positive neutrophils (Fig. 5M) were increased (cell numbers per 0.1 mm^2) in IL-33-treated mice whereas NICB3344 blocks these infiltrations. In addition, the protein levels of MPO were largely reversed in INCB3344-treated mice (Fig. 5N) in the hindpaw skin after IL-33 injection. These findings suggest that CCL2 rather than IL-33 itself could be the key chemoattractant to recruit those cells.

We then determined whether IL-33-induced pain hypersensitivity dynamically resolves as resolution of inflammation. The thermal hypersensitivity was resolved at day 1 and day 5 after IL-33 injection (Supplementary Fig. S5A–B). However, the infiltration of macrophages and neutrophils was still increased in the hindpaw skin in IL-33-treated mice at day 1 (Supplementary Fig. S5C–E). The infiltration of macrophages and neutrophils was largely reduced in IL33-treated mice at day 5 (Supplementary Fig. S5F–H). These data indicate that IL33-induced pain may be resolved before inflammation (macrophages and neutrophils) fading way.

IL-33-CCL2 facilitates pain states by activation of TRPs channels and enhancement of c-fiber-evoked LTP

Nociceptive sensory neurons fire by activation of ion channels or neurotransmitters. How IL-33-CCL2 signaling affects these neurons to instigate pain is the next key question. We examined gene expression of multiple ion channels in the hindpaw after IL-33 injection. The mRNA levels of *Nav1.7* (Supplementary Fig. S6A), *Nav1.9* (Supplementary Fig. S6B), *TRPA1* (Supplementary Fig. S6C) and *TRPM3* (Supplementary Fig. S6D) were unaltered in IL-33-treated mice. Interestingly, the mRNA levels of *TRPV1, TRPV4* and *TRPM8* were up-regulated in IL33-treated mice and this increase was largely reduced for *TRPV1* (Fig. 6A) and *TRPM8* (Fig. 6C) but not *TRPV4* (Fig. 6B) in *ST2−/−* mice. We also examined expressions of neurotransmitters such as Calcitonin Gene-Related Peptide (CGRP) and subsistence P (SP). There is a trend to increase *CGRP* (Supplementary Fig. S6E) but not *SP* (Supplementary Fig. S6F) in the hindpaw after IL-33 injection. As the up-regulation of *TRPV4* was not significantly reversed in *ST2−/−* mice after IL-33 injection, we focused on TRPV1 and TRPM8 in the following experiments. We further confirmed that TRPV1 and TRPM8 colocalizes with PGP9.5 (Fig. 6D) in skin nerve terminals. Blocking TRPV1 by intraperitoneal injection selective antagonist AMG9810 (200 μL, 30 mg/kg) 30 min before IL33 induction attenuates IL-33-induced mechanical (Fig. 6E) and thermal (Fig. 6F) hypersensitivity. In addition, intraplantar pre-treatment with another TRPV1 antagonist (capsazepine, CPZ,1 μg/20 μL) attenuated IL-33-induced thermal pain (Fig. 6G). Similarly, blocking TRPM8 channel with selective antagonist AMG2850 (1 μg/10 μL) reduces IL-33-induced cold allodynia (Fig. 6H). These data suggest that IL-33 induces pain hypersensitivity by activation of TRPV1 and TRPM8 in sensory neurons.

Whether IL-33-induced up-regulation of TRPV1 and TRPM8 is CCL2-dependent? We observed the expression of CCR2 in the hindpaw skin nerves (Fig. 6K). However, blocking CCR2 with INCB3344 was not sufficient to reverse IL-33-induced up-regulation of *TRPV1* (Supplementary Fig. S6G) and *TRPM8* (Supplementary Fig. S6H). In the CFA model, gene expressions of *TRPV1* (Supplementary Fig. S6I), *TRPM8* (Supplementary Fig. S6J) and *TRPV4* (Supplementary Fig. S6K) were not altered after CFA injection or in *IL33−/−* mice. These data suggest that the activation of TPRV1 and TRPM8 may not be CCL2-dependent in the hindpaw skin at periphery site. Using *CCL2−/−* mice may further help to identify whether TRPV1/TRPM8 activity is CCL2-dependent. We then examined mRNA levels of Nav channels, TRP channels and neurotransmitters in DRGs after IL-33 injection. Unfortunately, gene expression of *Nav 1.7* (Supplementary Fig. S7A), *Nav1.8* (Supplementary Fig. S7B), *Nav1.9* (Supplementary Fig. S7C), *TPRA1* (Supplementary Fig. S7D), *TRPV1* (Supplementary Fig. S7E), *TRPM3* (Supplementary Fig. S7F), *TRPV4* (Supplementary Fig. S7G), *TRPM8* (Supplementary Fig. S7H), *CGRP* (Supplementary Fig. S7I) and *SP* (Supplementary Fig. S7J) were unaltered. However, TRPV1-positive neurons were increased (Fig. 6I, J) in DRGs at 4 h after IL-33 injection while TRPM8-positive neurons were unaltered (Supplementary Fig. S7K, L). This indicates that IL-33 may also sensitize TRPV1-positive neurons in DRGs to cause pain.

How CCL2 interact with sensory neurons to accelerate pain progression? We detected expression of CCR2 at the nerve terminals (Fig. 6K). Intraplantar injection of CCL2 (200 ng/20 μL) induced robust mechanical (Fig. 6L) and thermal (Fig. 6M) hypersensitivity. We further recorded the c-fiber-evoked long-term potential (LTP) in the dorsal horn of spinal cord after intraplantar injection of IL-33, CFA or CCL2 in hindpaw of rats. As shown, PBS or IL-33 treatment does not elicit C-fiber-evoked field postsynaptic excitatory potentials (fEPSPs) (Fig. 6N), with (123.77 ± 7.78) % of c-fiber amplitude in PBS group and (103.73 ± 9.54) % in IL-33 group (Fig. 6O). However, CFA and CCL2 stimulation induced robust increase of c-fiber amplitude to (222.17 ± 15.33) % and (264.73 ± 30.05) % respectively (Fig. 6O) and pretreatment of INCB3344 reduced the CCL2-induced field potentials to

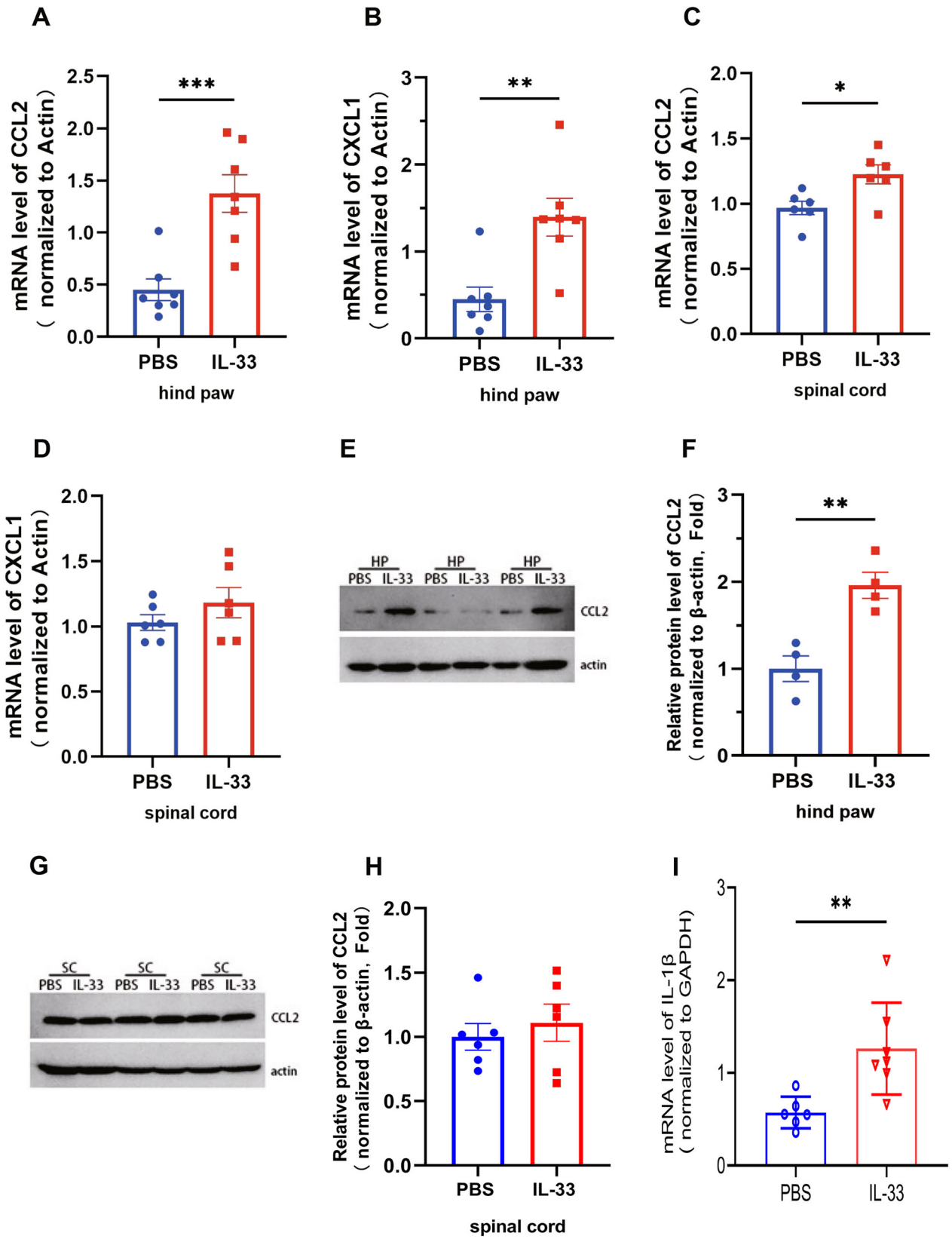

Fig. 3 | CCL2 was upregulated in the hindpaw in IL-33-treated mice. Gene expression of *CCL2* (**A**) and *CXCL*1 (**B**) was up-regulated at 4 h in the hindpaw in IL-33-treated mice (n = 7 mice). Gene expression of *CCL2* (**C**) but not *CXCL*1 (**D**) was up-regulated at 4 h in the spinal cord in IL-33-treated mice (n = 6 mice). **E** Western blots show the protein level of CCL2 at 4 h in the hindpaw in the IL-33 model. **F** Quantification of (**E**) (n = 4 mice). **G** Western blots show the protein level of CCL2 at 4 h in the spinal cord in the IL-33 model. **H** Quantification of (**G**) (n = 6 mice). **I** Gene expression of *IL1β* was up-regulated at 4 h in the hindaw in IL-33-treated mice (n = 6 mice). Data are presented as mean ± SEM. $^{*}p < 0.01$, $^{**}p < 0.01$, $^{***}p < 0.001$, Unpaired *t*-test for (**A**–**D**, **F**, **H**, **I**).

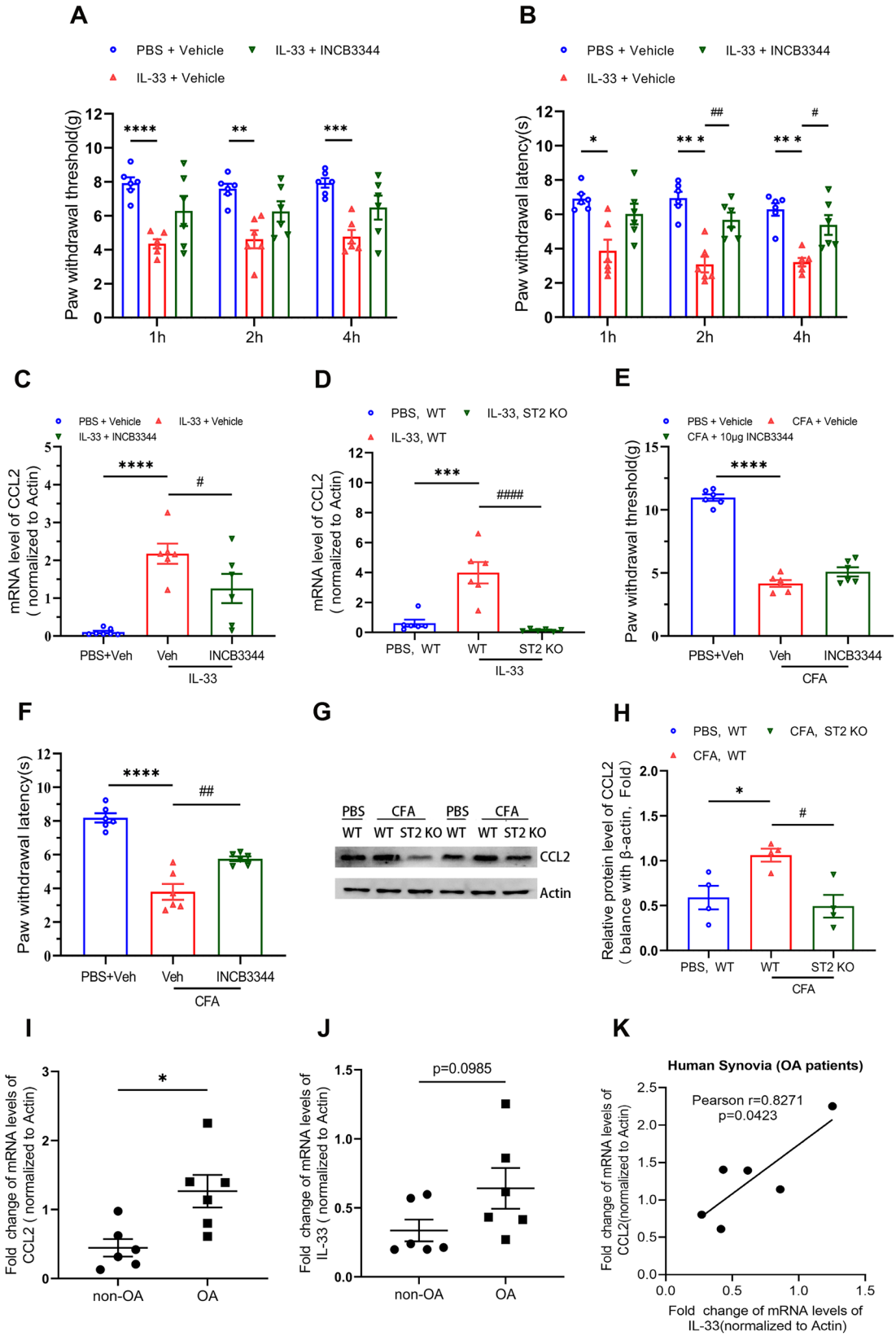

(131.61 ± 14.58) % (Fig. 6O). In addition, we performed the in-vivo recording of C-fiber evoked field potentials in the spinal dorsal horn to verify whether pretreatment with TRPV1 or TRPM8 antagonist by intraplantar injection can prevent LTP induced by intraplanar injection of CCL2. As shown, pretreatment with AMG9810 or AMG2850 largely reduced CCL2-induced LTP in spinal cord (Fig. 6P). The c-fiber amplitude was down-regulated from (252.86 ± 16.51) % in PBS group to (158.60 ± 15.57) % in AMG9810-treated group and (149.87 ± 10.30) % in AMG2850-treated group (Fig. 6P), suggesting essential role of TRPV1 and TRPM8 in CCL2-mediated neuronal activity. Together, these data

Fig. 4 | Blocking CCR2 attenuates IL-33-induced and CFA-induced thermal hyperalgesia in male mice. Pretreatment of CCR2 antagonist (INCB3344) does not affect mechanical allodynia (**A**) but reduces thermal hypersensitivity (**B**) in IL-33-induced pain (n = 6). **C** Gene expression of *CCL2* was partially reversed in the hindpaw of INCB3344-treated mice at 4 h after IL-33 application (n = 6 mice). **D** Gene expression of *CCL2* in the hindpaw in ST2−/− mice at 4 h after IL-33 application (n = 6 mice). Post-treatment of INCB3344 does not affect mechanical allodynia (**E**) but reduces thermal hyperalgesia (**F**) at day 3 after CFA injection (n = 6 mice). **G** Protein levels of CCL2 were down-regulated in the hindpaw in *ST2*−/− mice at day3 in the CFA model. **H** Quantification of (**G**) (n = 4 mice). **I** Gene expression of *CCL2* increased in the synovia of OA patients (n = 6 patients). **J** Gene expression of *IL-33* has a trend to increase in the synovia of OA patients (n = 6 patients). **K** Positive correlation between the gene expression of *IL-33* and gene expression of *CCL2* in the synovia of OA patients (n = 6 patients). Data are presented as mean ± SEM. $^{*}p < 0.01$, $^{**}p < 0.01$, $^{***}p < 0.001$, $^{\#\#\#}p < 0.001$. *represents PBS vs IL-33 or CFA in WT mice and #represents vehicle vs treatment or WT vs *ST2*−/− group in A-Fand H. Repeated measures for the two-way ANOVA with Bonferroni's post-hoc test for (**A**–**B**), One-way ANOVA with Bonferroni's post hoc test for (**C**–**F**, **H**), unpaired t-test for (**I**–**J**).

suggest that CCL2 may facilitate pain responses by enhancement of c-fiber-evoked LTP in the spinal cord in a TRPV1 and TRPM8-dependent manner.

Overall, our findings reveal an unrecognized neuroimmune crosstalk of immune cells and sensory neurons to drive inflammatory pain by the IL-33-CCL2 axis and activation of TRPV1 and TRPM8 channels.

Discussion

Pathogenic infection initiates host-defense and causes pain. However, how this natural process dynamically happens remains poorly understood. Here, we report that IL-33-CCL2 axis coordinates the neuroimmune crosstalk to drive pain via activation of TRPV1 and TRPM8 channels in the periphery and enhancement of c-fiber-evoked LTP in spinal cord.

The contribution of IL-33 to pain has been demonstrated in various models[22,44]. Nevertheless, most of the studies focus on a specific model and mainly target ST2 receptors as treatment in male animals. In this study, we examined function of IL-33 in acute and chronic pain using both male and female of *IL-33*−/− and *ST2*−/− mice. Intraplantar injection of IL-33 initiates acute mechanical, thermal and cold allodynia in both male and female mice. This acute pain is peaked at 4 h and recovers within 24 h[34] and global knockout of ST2 reduced IL-33-induced pain in both sexes. In the CFA model, mechanical allodynia and thermal hyperalgesia were attenuated in both male and female of *IL-33*−/− and *ST2*−/− mice at day 3 and day 9. In sexual-mixed samples from OA patients, the expression of IL-33 and ST2 was increased in the synovial fluid and cartilage[28]. We further found that MIA-induced mechanical allodynia was alleviated in the *ST2*−/− male mice and neutralizing ST2 receptor attenuated SNI-induced mechanical allodynia in both male and female mice[35]. Together, this suggests that IL-33/ST2 is essential for pain modulation in both male and female and could be a general therapeutic target for pain treatment.

IL-33 is a critical regulator for innate immunity, whether it initiates pain hypersensitivity via activation of ILC2s is interesting. We examined gene expression of type II cytokines in hindpaw skin after IL-33 injection. Unfortunately, the expression of *IL-4, IL-9*, and *IL-13* was neither altered in the hindpaw nor in spinal cord. This indicates ILC2s may not play a major role in IL-33-induced pain and a flow cytometry of these cells may strength this point. We then hypothesized that other inflammatory mediators may participate in IL-33-triggered pain. We screened a bunch of inflammatory mediators that were up-regulated in the FSL1 model[34]. We found that CCL2 was-upregulated in the hindpaw in IL-33-treated and CFA-treated mice, which was completely reversed in *ST2*−/− mice (Fig. 4D, H). Blocking CCR2 attenuates thermal hyperalgesia in both models (Fig. 4B, F), indicating CCL2 is the critical down-stream signal for IL-33-induced pain. To be noted, the up-regulation gene expression of CCL2 in the hindpaw was not reversed in the *IL-33*−/− mice in CFA model (Supplementary Fig. S3C), indicating other mediators may involve in CFA-induced pain processing. Overall, these data suggest that CCL2/CCR2 is required for IL-33-induced pain in both models.

We further examined whether this up-down link appears in osteoarthritic patients who normally have severe chronic pain. The gene expression of *CCL2* and *IL-33* increases while gene expression of *ST2* was not altered in synovia of OA patients, compared to non-OA patients. This was supported by other studies showing that the expression of *IL-33* and *CCL2* was up-regulated in both synovia and cartilage of OA patients[28,45]. Specifically, a positive correlation between *CCL2* and *IL-33* has been shown in synovia of OA patients but not in non-OA patients. No correlation was found for gene expression between *CCL2* and *ST2* in synovia or *CCL2* and *IL-33* in cartilage in OA patients. Together, these lines of evidence indicate a critical role of IL-33 and CCL2 in osteoarthritic pain and strengthens the link between those two signals in pain processing.

Where does CCL2 secrete from is the next interesting question. Co-staining CCL2 with MPO, F4/80 and tryptase suggests that CCL2 was mainly secreted by the infiltrated neutrophils, macrophages and mast cells but not resident keratinocytes or skin nerves in the hindpaw after IL-33 application. Ablation of macrophages reduces IL-33-induced pain responses and expression of CCL2 and ST2 in the hindpaw skin. Stimulation of macrophage cell-line (Raw246.7) with IL-33 for 24 h increases CCL2 secretion further support that IL-33 activates macrophages to release CCL2.

Blocking CCR2 inhibits infiltration of macrophages and neutrophils after IL-33 injection, indicating CCL2 as chemoattractant to these immune cells. This is supported by a line of evidence to show that CCL2 recruits macrophages to facilitate chronic pelvic pain, neuropathic pain and back pain[46–48] and blocking CCL2/CCR2 decreases macrophage infiltration and relieves cartilage damage in OA mouse model[45]. In addition, CCL2 also expresses in mast cells and stimulation of human mast cell with IL-33 has been shown to induce CCL2 secretion[49] and IL-33 administration increases CCL2 to promote the proliferation of decidual stromal cells[50]. These findings together suggest that CCL2 released by the innate immune cells is IL-33-dependent.

Neuronal regulation of immune cells is an emerging area for neuroimmune interaction. CGRP and SP have been involved in infiltration of immune cells[51]. We also detected their expression in the hindpaw skin at 4 h after IL-33 injection. The expression of *CGRP* has a tendency to increase (Supplementary Fig. S6E) while expression of *SP* is not altered (Supplementary Fig. S6F) in the IL-33-treated mice. At this point, it seems the neuropeptides may not affect infiltration of macrophages and neutrophils.

We further observed the effects of IL-33-induced pain for a longer period of time to see how this dynamic process happens. IL-33-induced pain was resolved within 24 h, whereas the resolution of neutrophils and macrophages was delayed until day 5. This indicates that pain responses may not be resolved exactly as resolution of inflammation.

How IL-33-CCL2 ultimately affects sensory neurons in the periphery is intriguing. Screening a series of ion channels expressing in the hindpaw skin, we found the gene expression of *TRPV1, TRPV4*, and *TRPM8* channels rather than *TRPA1* and *TRPM3* channels nor *Nav1.7/Nav1.9* channels were increased after IL-33 application. The increase of *TRPV1* and *TRPM8* was reversed in the *ST2*−/− mice (Fig. 6A, C). Indeed, TRPV1 and TRPM8 were detected in skin nerve terminals. Though we cannot exclude that TRPV1 and TRPM8 may express in other cells such as keratinocytes[52], blocking TRPV1 attenuated IL-33-induced mechanical and thermal hypersensitivity and blocking TRPM8 relieves IL-33-induced clod allodynia. These results suggest that IL-33 causes pain via activation of TPRV1 and TRPM8 channels. We also detected TRPV1 and TRPM8 in DRG neurons and found that TRPV1-positive but not TRPM8-positive neurons were increased in DRG neurons after IL-33 application. However, a recent study shows that ST2 colocalizes with TRPM8 neurons in DRGs in SNI mice and rIL-33 activates these neurons to mediate cold allodynia[53]. Interestingly, another study revealed that IL-33 recruits neutrophils to release reactive oxygen species,

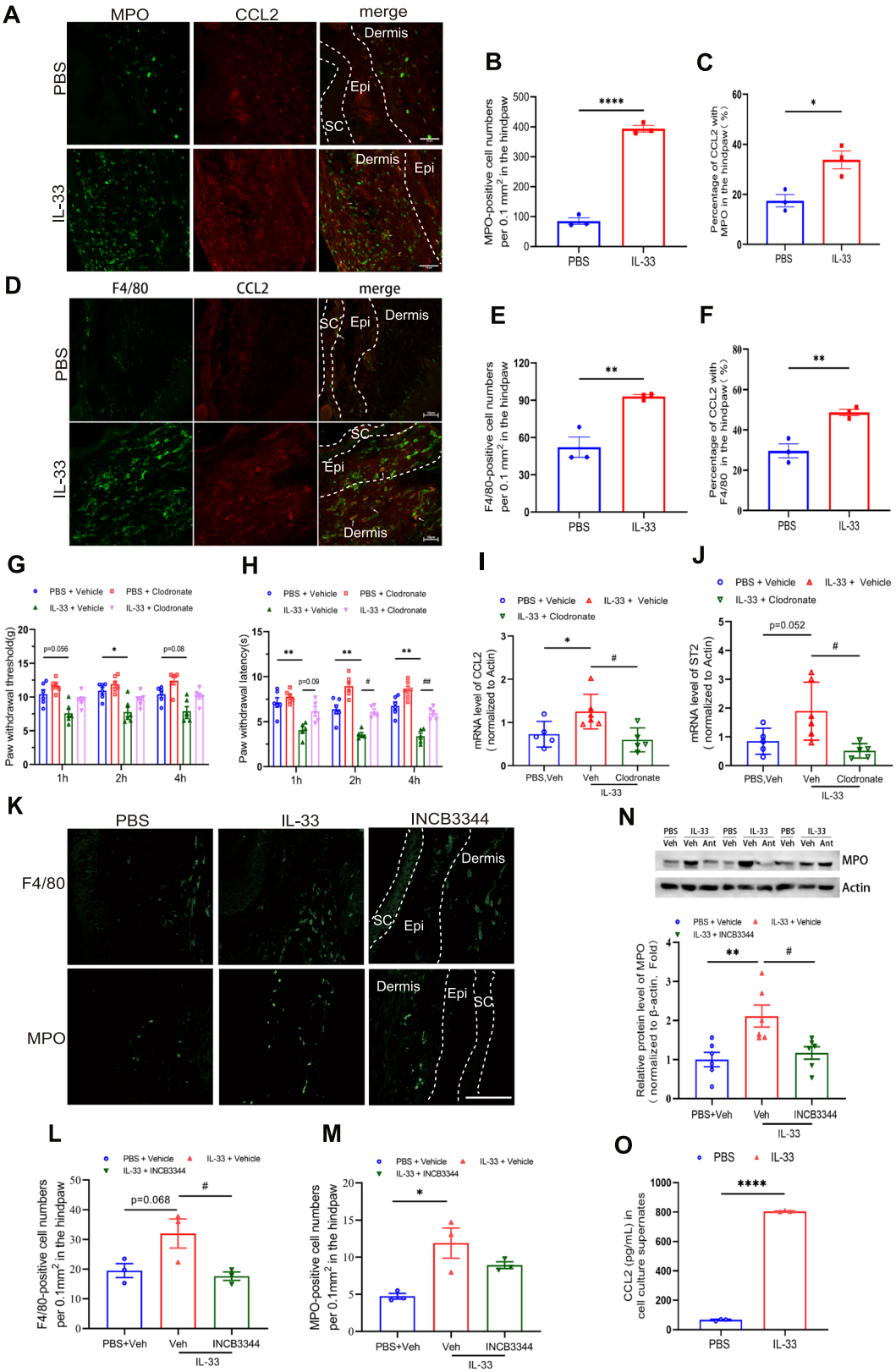

which activates TRPA1 in DRG neurons in the gout pain[27], suggesting that IL-33 may induce pain also via activation of TRP channels in DRG neurons.

We further examined whether the up-regulation of TRPV1 and TRPM8 is CCL2-depdent. Unfortunately, the up-regulation of mRNA levels of *TRPV1* and *TRPM8* was not diminished by CCR2 antagonist in the hindpaw skin in IL-33-induced and CFA-induced model. Nevertheless, TPRV1-positive neurons were increased in DRGs after IL-33 injection, which may be sensitized by CCL2. Indeed, intraplantar pretreatment with TRPV1 antagonist or TRPM8 antagonist prevents CCL2-induced LTP in spinal cord (Fig. 6P). Furthermore, others show that CCR2 colocalizes with

Fig. 5 | CCL2 is released by macrophages and neutrophils in vivo and in vitro with IL-33 stimulation. A Co-localization of CCL2 with neutrophil marker (MPO) in the hindpaw skin at 4 h after IL-33 injection (n = 3 mice, scale bar: 50 μm). Quantification of (**A**) for neutrophil infiltration (**B**) and percentage of neutrophils expressing CCL2 (**C**) (n = 3 mice). **D** Co-localization of CCL2 with macrophage marker(F4/80) in the hindpaw skin at 4 h after IL-33 injection (n = 3 mice, scale bar: 50 μm). Quantification of (**D**) for macrophage infiltration (**E**) and percentage of macrophages expressing CCL2 (**F**) (n = 3 mice). Depletion of macrophages by intraperitoneal injection of Clodronate liposome (i.p: 200 μl, once a day for 2 days) attenuates IL33-induced mechanical (**G**) and thermal (**H**) hypersensitivity (n = 5-6 mice). Depletion of macrophages by intraplantar injection of Clodronate liposome (i.p: 200 μl) reverses gene expression of *CCL2* (**I**) and *ST2* (**J**) (n = 5-6 mice). **K** Infiltration of macrophages and neutrophils after CCR2 blocking (n = 3 mice, scale bar: 100 μm). Quantification for infiltration of macrophages (**L**) and neutrophils (**M**) after CCR2 blocking in the IL-33 model. **N** Western blots and quantification of protein levels of MPO in the hindpaw of INCB3344-treated mice at 4 h after IL-33 injection. (n = 6 mice). **O** IL-33 stimulation increases CCL2 secretion from the Raw264.7 cells in 24 h (n = 3 trials). Data are presented as mean ± SEM. $^{*}p < 0.05$, $^{**}p < 0.01$, $^{***}p < 0.001$, $^{****}p < 0.0001$, $^{\#}p < 0.05$. $^{\#}$represents vehicle vs drug treatment. Unpaired *t*-test for (**B**, **C**, **E**, **F**, **O**), One-way ANOVA with Bonferroni's post-hoc test for (**I**, **J**, **L**–**N**), Repeated measures for two-way ANOVA with Bonferroni's post-hoc test for (**G**–**H**). The skin layers are stratum corneum (SC), epidermis (Epi) and Dermis.

TRPV1-positive neurons in DRGs and activation of CCR2 sensitized TRPV1 channels[54]. Incubation of DRG neurons with CCL2 increases mRNA level of TRPV1 and Nav1.8[38] and blocking TRPV1 channel inhibited CCL2-induced EPSC in the spinal cord and thermal hyperalgesia[55]. These findings together support that CCL2/CCR2 axis may activate TRPV1 to promote pain. Using *CCL2* knockout mice will be good way to confirm this in future study.

Lastly, we recorded c-fiber-evoked LTP in the dorsal horn of spinal cord with IL-33, CCL2 or CFA injection in the hindpaw. Intraplantar injection of IL-33 itself does not induce LTP in naïve rats, however application of CCL2 or CFA induces enhanced LTP in the spinal cord. Blocking CCR2 prevents CCL2-induced LTP. These results further suggest that IL-33 requires CCL2 as down-stream signals to elicit the neuronal firing and pain.

Altogether, we reveal the synergic crosstalk of IL-33-CCL2 signals from infiltrated neutrophils and macrophages interact with TRPV1 and TRPM8 in sensory neurons to facilitate transition of pain states.

Methods

Animals

Animal protocols were approved by the Institutional Animal Care and Use Committee at Sun Yat-sen University (approval number: SYSU-IACUC-2020-B1206) and conform to IASP Guidelines for the Use of Animals in Research. C57BL/6 J mice and Sprague Dawley (SD) rats were obtained from Laboratory Animal Center at Sun Yat-sen University and Guangdong Medical Laboratory Animal Center. IL-33–deficient (*IL33* +/−) mice and ST2-deficient (*ST2*+/−) mice with C57/6 J as genetic background were gifted by Dr WL. Mi at Shanghai Medical College, Fudan University and were in-house breaded and generated at Laboratory Animal Center of Sun Yat-sen University. All mice and rats were used for experiments between 7-12 weeks. Animals were kept on a 12-hr light/dark cycle and at a temperature of 23 ± 1 °C; food and water were available *ad libitum*.

Mouse genotyping

Mouse ear or tail tissues were harvested and digested by lysis buffer containing proteinase K. The mixture was incubated at 56 °C for 15 min and 95 °C for 1 h. After the digestion, samples were cooled down to 4 °C and balanced buffers were added, mixed and centrifuged to get DNA samples. Then PCR mix was setup and PCR reaction was run at 95 °C for 2 min, followed by 35 cycles at 95 °C(30 s) − 60 °C(30 s) − 72 °C(30 s). After PCR amplification, samples were continued to run by gel electrophoresis. The primers are as follows: *ST2*: TTGGCTTCTTTTAATAGGCCC (primer1), CTATCAGGACATAGCGTTGGCTACC (primer2), TGTTGAAGC-CAAGAGCTTACC (primer3) and *IL-33*: CACTAAGACTACTCAGC CTCAG (primer1), CGGTGATGCTGTGAAGTCTG (primer2), GTGTT CTGCTGGTAGTGGTCG (primer 3).

Animal models for pain

Several pain models were used in this study. For the IL-33 model, recombinant mouse IL-33 (3626-ML/CF, 200 ng/20 μL) or PBS was intraplantarly injected into the left hind paw. Paw withdrawal threshold (PWT) or Paw withdrawal latency (PWL) was measured at 4 h post injection. For the CFA model, 20 μL of CFA (F5881, Sigma-Aldrich) or PBS was intraplantarly injected into the left hind paw. Then mechanical PWT or thermal PWL was measured at day 3 and day 9 after CFA injection. For the MIA model, MIA (0.2 mg/10 μL, I9148, Sigma-Aldrich) or PBS was intraarticular injected into the left knee and PWT was measured with a time-course from day 1 to day21. For the CCL2 model, recombinant mouse CCL2 (200 ng/20 μL, 479-JE/CF, R&D) or PBS was intraplantar injected into the left hindpaw. then mechanical PWT or thermal PWL was measured at 1,2,4 and 6 h after CCL2 injection.

Behavioral testing for nociception

Animals were randomly assigned to each group. Mice were habituated in chambers for at least 60 min before testing. Mechanical PWT was measured using electrical von Frey (Bioseb BIO-EVF4-S, France). Mice were individually placed in a plexiglass chamber (20 cm × 18.5 cm × 13 cm, length × width × height) over a wire mesh floor. The aesthesiometer was placed under the hind paw with the filament directly stimulating the central plantar surface of the hind paw. Paw withdrawal threshold was tested 3–5 times with at least 3 min intervals between each stimulation. Thermal latency was measured by using a Hargreaves glass platform (UgoBasile, Varese, Italy). The hindpaw withdrawal latency from a focused beam of radiant heat was recorded and each paw was tested for 3–5 times with at least 5 min intervals between each testing. Radiant heat was set to no more than 30 s to avoid tissue damage of the hind paw.

Drug treatment in pain models

In the pre-treatment study, ST2 neutralizing antibody (0.5 μg/10 μL, MAB10041, R&D), CCR2 antagonist (INCB3344, 0.5 μg/10 μL, Apebio) or PBS was intraplanatarly delivered 30 min before IL-33 injection. Then mechanical PWT or thermal PWL was measured at 1, 2, and 4 h after IL-33 injection. For the post-treatment study, CFA model was set up and INCB3344 was intraplantarly injected at day 3 after CFA injection, then PWL was measured. For the macrophage depletion experiment, clondronate (200 μL, CP-005-005, Liposoma) was intraperitoneal injected once a day for two days, then IL-33 was intraplantarly injected. PWT and PWL were measured at 1, 2, and 4 h after IL-33 application.

For TRPV1 blocking experiments, TRPV1 antagonist-AMG 9810 (MCE, HY-101736) was intraperitoneally (200 μL, 30 mg/kg) injected 30 min before IL33 (3626-ML/CF, 200 ng/20 μL) injection. Thermal hyperalgesia and mechanical allodynia were measured 1 h after IL-33 injection. The capsazepine (CPZ, MCE, HY-15640), another TRPV1 antagonist, was intraplantarly injected (0.3 μg/20 μL,1 μg/20 μL) into the left hindpaw 30 min before IL-33 injection. Then thermal PWL was measured at 1, 2, and 4 h after IL-33 injection.

Animals were randomly assigned to each group and all the treatments and behavioral tests were double-blinded.

Cold allodynia test

For the IL-33 model. IL-33 was intraplantarly injected to the left hindpaw. Cold allodynia was assessed using the acetone evaporation test as literature reported with minor modifications[56,57]. Mice were habituated for 45 min in observation chambers on a floor grid mesh platform. Briefly,

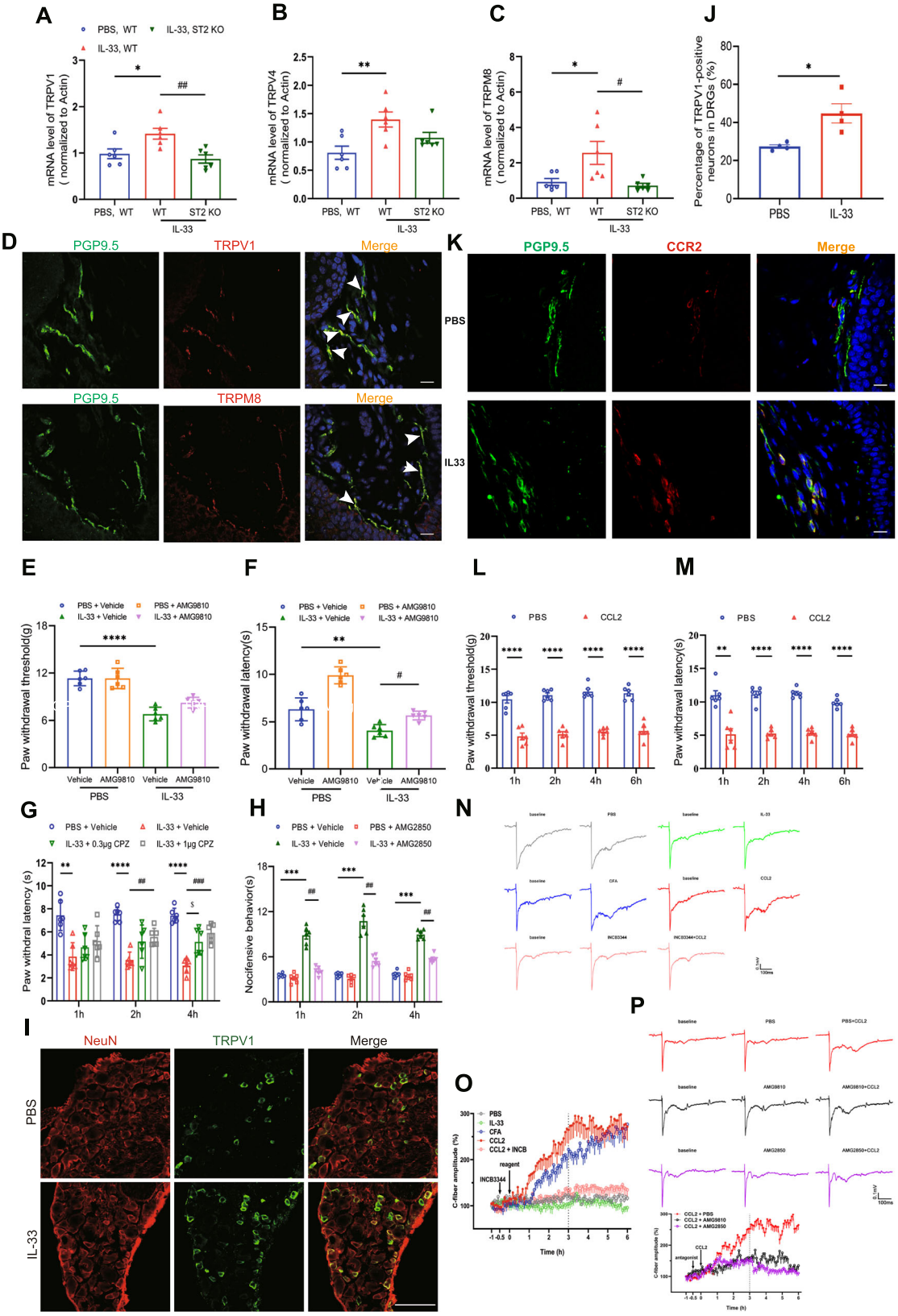

20 μL acetone was applied to the plantar surface of the left hindpaw with a 0.5 mL syringe. The cumulative time of nocifensive behaviors (paw withdrawal, licking, or flinching) was observed, and the behavior was quantified for 1 min after acetone application using a chronometer. Three measurements were performed for each mouse, with 5 min intervals between each acetone instillation. The mean of three measurements was calculated as the nocifensive behavior time (s). An increase of nocifensive response was considered cold allodynia. For TRPM8 antagonist experiment, AMG2850 (1 μg/10 μL, MCE, HY-104059) or 10 μL vehicle was intraplantarly delivered 30 min before IL-33 injection (3626-ML/CF,

Fig. 6 | IL-33-CCL2-induced pain hypersensitivity is mediated by the up-regulation of TRP channels in the hindpaw and enhancement of c-fiber- evoked LTP in the spinal cord. (**A**–**C**) Gene expression of *TRPV1* (**A**), *TRPV4* (**B**) and *TRPM8* (**C**) in the hindpaw skin in *ST2*−/− mice at 4 h after IL-33 injection (n = 5-7 mice). **D** Colocalization of TRPV1(upper panel) and TRPM8(lower panel) with PGP9.5 in the hindpaw (n = 3 mice, scale bar: 100 μm). Blocking TRPV1 with AMG9810 attenuated IL-33-induced mechanical (**E**) and thermal hypersensitivity (**F**) (n = 6 mice). **G** Blocking TRPV1 with capsazepine (CPZ) attenuated IL-33-induced thermal hypersensitivity (n = 6 mice). **H** Blocking TRPM8 with AMG2850 attenuated IL-33-induced cold allodynia (n = 6). **I** Expression of TRPV1 in DRGs (n = 3 mice, scale bar: 100 μm). **J** Quantification of (**I**), TRPV1-postive number in DRGs(n = 3 mice). **K** Colocalization of CCR2 with PGP9.5 in the hindpaw (n = 3 mice, scale bar: 100 μm). Intraplantar injection of CCL2 induces mechanical (**L**) and thermal hypersensitivity (**M**) (n = 6 mice). **N** Representative LTP traces show c-fiber-evoked field potentials in the dorsal horn of spinal cord in various inflammatory pain models. **O** Quantification of (**N**) (n = 5 rats). **P** Representative LTP traces show c-fiber-evoked field potentials in the dorsal horn of spinal cord by pretreatment with AMG9810 and AMG2850 in CCL2-induced model (n = 3 rats). Data are presented as mean ± SEM. $^{*}p < 0.01$, $^{**}p < 0.01$, $^{****}p < 0.0001$, $^{\#}p < 0.05$, $^{\#\#}p < 0.01$, $^{\#\#\#}p < 0.001$, $^{\#\#\#\#}p < 0.0001$, $^{\$}p < 0.05$, $^{\$\$}p < 0.01$, $^{\$\$\$\$}p < 0.0001$. $^{\#}$g represents WT vs ST2−/− or vehicle vs drug treatment and $^{\$}$represents PBS+veh vs IL-33+drug treatment (0.5 μg CPZ in (**G**) or AMG2850 in (**H**)). One-way ANOVA with Bonferroni's post-hoc test for (**A**–**C, E, F**), unpaired t-test for (**J, O, P**), Repeated measures for two-way ANOVA with Bonferroni's post-hoc test for (**G, H, L, M**).

200 ng/20 μL). Then cold allodynia was measured at 1, 2, and 4 h after IL-33 injection.

SYBR Green quantitative real-time polymerase chain reaction (qRT-PCR)

After behavioral testing, mice were euthanized with isofluorane. Fresh hindpaw and dorsal horn of ipsilateral spinal cords were collected and stored at −80 °C. Tissues were homogenized in ice cold TRI-reagents to extract total RNA from the samples following manufacture's instruction. Primers were designed at NCBI and synthesized by IGE Biotechnology LTD (Guangzhou, China). The sequences are as follows:

β-actin Fw: ACCCGCGAGCACAGCTTCT, Rv: GCCTCGTCACCCACATAGGAGTCC

IL-4 Fw: AACGAGGTCACAGGAGAAGGGA, Rv: TTGGAAGCCCTACAGACGAGC

IL-9 Fw: AACATCACGTGTCCGTCCTT, Rv: TGCCTTTGCATCTCTGTCTTCT

*IL-13*Fw: TCTGTGTCTCTCCCTCTGACCC, Rv: GGAATCCAGGGCTACACAGAAC

IL-17 Fw: CCAAACACTGAGGCCAAGGA, Rv: AGGGTCTTCATTGCGGTGGA

CCL2 Fw: GCAGGTCCCTGTCATGCTTC, Rv: GGCGTTAACTGCATCTGGCT

*CXCL1*Fw: CCAAACCGAAGTCATAGCCACA, Rv: GAACCAAGGGAGCTTCAGGG

*CCL12*Fw: ATTGGCTGGACCAGATGCG, Rv: CCGGACGTGAATCTTCTGCTT

*TRPV1*Fw: GTGGTGCTTCAGGGTGGATG, Rv: CTCACAGTTGCCTGGGTCCT

*TRPV4*Fw: GACATCGAGCGTTCCTTCCC, Rv: TCACCTCGTCCACCCTGAA

*TRPM3*Fw: AGCAGACACCGGCTCAGAA, Rv: TATGAGGCGTCCACAGCAAC

TRPM8 Fw: TACATCGCCTTCCTCCTGCT, Rv: CCGTTCATGTACCACTGCCT

*TRPA1*Fw: CCACAATGGCTGGACTGCTT, Rv: AGTGGAGTGCTGTGTTCCCT

*Nav1.7*Fw: TGTCCAAGTCAGGGTCAGAGG, Rv: GCTGAGTGGTGACTGGTTGG

Nav1.9 Fw: CAGCATTGTGGCCCTTGTGA, Rv: ACTTGAAGACCCTCAGCACTCT

*Tac1(SP)*Fw: AGTGACCAGATCAAGGAGGCA, Rv: CTGCTGAGGCTTGGGTCTTC

*CGLCA(CGRP)*Fw: CCCTTTCCTGGTTGTCAGCA, Rv: TGGGCTGCTTTCCAAGA

TTGA.

For q-PCR in DRG, some primers were designed by another experimenter. The sequences are as follows:

*TRPV1*Fw: ACACCATTGCTCTGCTCCTG, Rv: TGTAATGCTGTCTGGCCCTTG

TRPM3 Fw: AGCAGACACCGGCTCAGAA, Rv: TATGAGGCGTCCACAGCAAC

TRPM8 Fw: CCCGAGCAGTGGAGTTGTTC, Rv: CAGCTCCAGACAGTTGCTCC

*TRPA1*Fw: TGCTGAGATCGACCGGAGTG, Rv: GGGTGCTGAAGGCATCTTGG

Nav 1.8 Fw: GCTGTACCAGCAGACACTCC, Rv: GTTGCCTGGCTCTGTTCCTC

Tac1(SP) Fw: AGTGACCAGATCAAGGAGGCA, Rv: CTGCTGAGGCTTGGGTCTTC

CGLCA(CGRP) Fw: AGATCCTGCAACACTGCCAC, Rv: ACCACACCTCCTGATCT

GCT. *IL1β* Fw: GGATTGAGGTTGCTCTGTTCTGG, Rv: ATCGTAGAGCTTGCCATC

GTTC. *GAPDH* Fw: TGTGTCCGTCGTGGATCTGA, Rv: TTGCTGTTGAAGTCGCA

GGAG.

250 ng of RNA was reversely transcribed with Transcript Uni All-in-One First-Strand cDNA Synthesis Kit (AU341, TransGen Biotech, China) following the manufacturer's instructions. cDNA synthesis was conducted at 50 °C for 5 min to synthesize cDNA and 85 °C for 5 s to inactivate the reaction. cDNA samples were amplified by PerfectStart Green qPCR SuperMix (AQ601, TransGen Biotech, China). The PCR reaction started at 94 °C for 30 s, followed by 40 cycles at 94 °C for 5 s, 55 °C for 15 s and 72 °C for 10 s.

Human samples for qRT-PCR

Human samples were consented by the participants and collected from Orthopedic Hospital of Guangdong Province. The protocol was approved by ethic committee for clinical trials (approval number:2023-伦理-064). 10 female late OA patients and 9 (6 male and 3 female) non-OA patients with Meniscus injury, ACL or both were recruited. The age of OA patients is between 51 to 95 while non-OA patients are younger with age from 25 to 60 years old. 3 OA patients and 3 non-OA patients who have ever used analgesic drugs were excluded for qPCR testing. The fresh synovia and cartilages were collected, snap frozen in liquid nitrogen and transferred to −80 °C. RNA was extracted by SteadyPure RNA (AG21022, AG21024, Accurate Biology, China) and 250 ng of RNA was reversely transcribed by Evo M-MLV master mix (AG11mix, Accurate Biology, China) following the manufacturer's instructions. cDNA samples were amplified by PerfectStart Green qPCR SuperMix (AQ601, TransGen Biotech, China). The PCR reaction started at 94 °C for 30 s, followed by 40 cycles at 94 °C for 5 s, 55 °C for 15 s and 72 °C for 10 s. The gene expression of IL-33, CCL2 and ST2 was quantified and the gene sequences are as follows: Human *β-actin* Fw : TGGCACCCAGCACAATGAA, Rv: CTAAGTCATAGTCCGCCTAGAAGCA; Human *IL-33* Fw: TGGAGTGCTTTGCCTTTGGT, Rv: CCATCAACACCGTCACCTGATT; Human *CCL2* Fw: GAAAGTCTCTGCCGCCCTT, Rv: GGGCATTGATTGCATCTGGC T. Human *ST2* Fw: TCACGGTCAAGGATGAGCAA, Rv: ACGGCAGCCAAGAACTGA. The expression levels of all the genes were normalized to *β-actin*.

Western Blot analysis

Fresh hindpaw tissues or spinal cord were harvested and stored in −80 °C. Samples were homogenized in the RIPA buffer containing protease and

phosphatase inhibitors (Roche), and were sonicated and centrifuged at 12,000 g for 15 min at 4 °C. The supernatants were transferred to fresh tubes and protein concentrations were assayed by Pierce BCA Protein Assay Kit (Thermofisher, 23227) following manufacturer's instructions. The samples were mixed with SDS-PAGE Protein Sample Loading Buffer (5X, P0015, Beyotime, China) in 4:1 and were boiled for 5 min at 100 °C. The gels were made by SDS-PAGE Gel Quick Preparation Kit (P0012AC, Beyotime, China). The samples were separated by SDS-PAGE and transferred onto PVDF membranes. The membranes were blocked with 5% non-fat milk (1706404, BIO-RAD) in PBS and were incubated with primary antibodies (Myeloperoxidase, Abcam, ab208670; CCL2, Proteintech, 66272-1-Ig;CCR2, Abcam, ab273050; β-actin, Bioworld, AP0060) overnight at 4 °C, followed by HRP-conjugated Goat anti-Mouse (bs-0368G-HRP, Bioss, China), Goat anti-Rat (bs-0293G-HRP, Bioss, China) and Goat anti-Rabbit (bs-0295G-HRP, Bioss, China) secondary antibodies. Immunoreactive bands were visualized with an ECL enhanced chemiluminescence detection kit (WBKLS0100, Millipore) using the Chemidoc Touch Imaging System (Bio-Rad). The immunoblots was analyzed by Fiji (ImageJ).

Raw264.7 cell culture with IL-33 stimulation

The Raw264.7 cells were cultured in Dulbecco's modified Eagle's medium (DMEM) supplemented with 10% fetal bovine serum and 1% antibiotic-antimycotic (10,000 IU/mL penicillin, 10,000 μg/mL streptomycin, 15-140-122, Gibco, USA). Cells were maintained in a humidified incubator with 95% air and a 5% CO2 atmosphere at 37 °C. For the IL-33 stimulation, cells were seeded on a 6-well plate with DMEM for overnight. The DMEM was removed, and cells were washed with PBS for 2–3 times next day. New DMEM containing IL-33 (50 ng/mL) or vehicle (PBS) was added immediately, and cells were cultured for another 24 h. After that the cultured supernatants were then harvested at the third day of cell culture and stored in −20 °C for future use.

Enzyme-linked Immunosorbent (ELISA) assay to quantify CCL2 secretion

To quantify the secretion of CCL2 in the supernatants from cultured Raw264.7 cells with IL-33 stimulation, the Mouse CCL2/JE/MCP-1 Quantikine ELISA Kit (R&D, USA) was used following the manufacturer's instructions. Briefly, 50 μL of RD1W and 50 μL of sample were added into the wells and were incubated for 2 h at room temperature (RT). The mixture was washed 5 times and 100 μL of MCP-1 linker was added and incubated for 2 h at RT. Washing 5 times and 100 μL of substrate was added and incubated for 0.5 h at RT. The reaction was terminated and quantification of CCL2 was determined by Absorbance microplate reader (Tecan Sunrise, Switzerland). For IL-33 measurement in blood, recombinant mouse IL-33 (3626-ML/CF, 200 ng/20 μL) or PBS was intraplantarly injected into the left hind paw. Serum was collected at 3–4 h post intraplantar injection and was measured by ELISA kit for IL-33 (Cloud-Clone Corp, SEB980Mu, China).

Immunohistochemistry

The immunostaining was performed as follow: Animals were transcardially perfused with PBS and 4% paraformaldehyde. Hindpaw tissues were harvested and post-fixed overnight at 4 °C fridge. Tissues were dehydrated in 20% and 30% sucrose for 24 h respectively, embedded in OTC and kept in −80 °C. The sections were permeabilized with 0.3% Triton X-100, blocked by 5% normal donkey serum and then were incubated overnight at 4 °C with the following primary antibodies: anti-CCL2 (mouse, 1:400, Proteintech, 66272-1-Ig), anti-CCR2 (rabbit, 1:200, Abcam, ab273050), anti-F4/80 (rat,1:200, Abcam, ab6640), anti- Myeloperoxidase (rabbit,1:400, Abcam, ab208670), anti-cytokeratin 14 (rabbit,1:200, Proteintech,10143-1-AP), anti-PGP9.5(mouse, 1:200, Abcam, ab8189; rabbit, 1:200, PGP9.5 GTX109637), Anti-MCP1(rabbit,1:200, Abcam, Ab25124), Mast Cell Tryptase (mouse, 1:200, AbcamAb2378), ST2 Polyclonal Antibody (rabbit,1:500, Thermo Fisher Scientific, PA5-20077), Anti-TRPV1 (rabbit, 1:200, Abcam, Ab6166) and TRPM8 Polyclonal antibody (rabbit,1:100, ProteinTech,12813-1-AP). After washing, the sections were incubated for 1 h at RT with the following secondary antibodies, purchased from Thermofisher (Alexa Flour 488/546, A-21206, A-21208, A-10036). Images were visualized and captured on a Zeiss LSM800/Leica DM6B and processed identically.

C-fiber-evoked field potentials recording

Animals were anesthetized with urethane (1.5 g/kg, i.p.). The trachea was cannulated, letting the animal breath spontaneously. Lumbar enlargement of spinal cord was exposed, and the dura mater was incised longitudinally. The left sciatic nerve was dissected freely for bipolar electrical stimulation. After all the above preparation the animals were placed on a stereotaxic apparatus. The left sciatic nerve was covered with warm paraffin oil. CCR2 antagonist (INCB3344, 1 ug/100 μL), TRPV1 antagonist (AMG9810, 100 ug/100 μL) or TRPM8 antagonist (AMG2850, 30 ug/100 μL) was intraplantarly injected 0.5 h before CCL2 injection (1 ug/100 μL). Recording of C-fiber evoked field potentials in the spinal dorsal horn was done as described previously[58,59]. Briefly, the exposed left sciatic nerve was electrically stimulated with a bipolar silver chloride hook electrode, and field potentials were recorded 100–500 μm deep from the surface of the spinal cord in the ipsilateral lumbar enlargement with a glass microelectrode (impedance 2–4 MΩ, contained 0.5 M sodium acetate as pipette solution), driven by an electronically controlled microstepping motor (Narishige Scientific Instrument Laboratory). An A/D converter card (National Instruments M-Series PCI express) was used to digitize and store data at a sampling rate of 10 kHz in the computer. The amplitudes of C-fiber evoked field potentials were determined on-line by LTP program (Ver 2.30D, William W. Anderson, http://www.winltp.com/). In each experiment, LTP was recorded for 6 h and amplitudes of 5 consecutive field potentials recorded at 1 min interval were averaged. The mean amplitude of averaged responses before intraplantar injection of reagent served as baseline control. To calculate LTP, the amplitude of C-fiber-evoked field potentials was normalized to the mean baseline amplitude.

Statistics and reproducibility

Data were analyzed with Graphpad Prism 8.0/9.0 and Image J and are presented as the mean ± SEM. Gene expression data were analyzed by unpaired *t*-test. In vivo data were analyzed by unpaired *t*-test, one-way or Repeated measures for two-way analysis of variance (ANOVA) with Bonferroni post-hoc correction or paired *t*-test. For immunofluorescence, data were analyzed by one-way ANOVA with Bonferroni post-hoc correction or unpaired *t*-tests. Statistical significance was accepted at the level of $p < 0.05$.

Data availability

The data sets generated and/or analyzed during the current study are available upon reasonable request from the corresponding author. Uncropped gel images and the gray value of the bands are provided in Supplementary Information.

Received: 18 September 2024; Accepted: 22 April 2025;
Published online: 10 May 2025

References

1. Ji, R. R., Xu, Z. Z., Strichartz, G. & Serhan, C. N. Emerging roles of resolvins in the resolution of inflammation and pain. *Trends Neurosci.* **34**, 599–609 (2011).
2. Ji, R. R. Specialized pro-resolving mediators as resolution pharmacology for the control of pain and itch. *Annu. Rev. Pharmacol. Toxicol.* **63**, 273–293 (2023).
3. Nicotra, L., Loram, L. C., Watkins, L. R. & Hutchinson, M. R. Toll-like receptors in chronic pain. *Exp. Neurol.* **234**, 316–329 (2012).
4. Liu, T., Gao, Y. J. & Ji, R. R. Emerging role of Toll-like receptors in the control of pain and itch. *Neurosci. Bull.* **28**, 131–144 (2012).
5. Acioglu, C., Heary, R. F. & Elkabes, S. Roles of neuronal toll-like receptors in neuropathic pain and central nervous system injuries and diseases. *Brain Behav. Immun.* **102**, 163–178 (2022).

6. Zhang, H. et al. The inflammasome as a target for pain therapy. *Br. J. Anaesth.* **117**, 693–707 (2016).
7. Chen, R., Yin, C., Fang, J. & Liu, B. The NLRP3 inflammasome: an emerging therapeutic target for chronic pain. *J. Neuroinflamm.* **18**, 84 (2021).
8. Baekkevold, E. S. et al. Molecular characterization of NF-HEV, a nuclear factor preferentially expressed in human high endothelial venules. *Am. J. Pathol.* **163**, 69–79 (2003).
9. Schmitz, J. et al. IL-33, an interleukin-1-like cytokine that signals via the IL-1 receptor-related protein ST2 and induces T helper type 2-associated cytokines. *Immunity* **23**, 479–490 (2005).
10. Martin, N. T. & Martin, M. U. Interleukin 33 is a guardian of barriers and a local alarmin. *Nat. Immunol.* **17**, 122–131 (2016).
11. Dwyer, G. K., D'Cruz, L. M. & Turnquist, H. R. Emerging functions of IL-33 in homeostasis and immunity. *Annu. Rev. Immunol.* **40**, 15–43 (2022).
12. Han, P., Mi, W. L. & Wang, Y. Q. Research progress on interleukin-33 and its roles in the central nervous system. *Neurosci. Bull.* **27**, 351–357 (2011).
13. Fairlie-Clarke, K. et al. Expression and function of IL-33/ST2 Axis in the central nervous system under normal and diseased conditions. *Front. Immunol.* **9**, 2596 (2018).
14. Sun, Y. et al. Therapeutic opportunities of interleukin-33 in the central nervous system. *Front. Immunol.* **12**, 654626 (2021).
15. Mamuladze, T. & Kipnis, J. Type 2 immunity in the brain and brain borders. *Cell Mol. Immunol.* **20**, 1290–1299 (2023).
16. Fu, A. K. et al. IL-33 ameliorates Alzheimer's disease-like pathology and cognitive decline. *Proc. Natl. Acad. Sci. USA* **113**, E2705–E2713 (2016).
17. Saresella, M. et al. IL-33 and its decoy sST2 in patients with Alzheimer's disease and mild cognitive impairment. *J. Neuroinflamm.* **17**, 174 (2020).
18. Liu, X. et al. Regulatory T cell is critical for interleukin-33-mediated neuroprotection against stroke. *Exp. Neurol.* **328**, 113233 (2020).
19. Yang, Y. et al. ST2/IL-33-dependent microglial response limits acute ischemic brain injury. *J. Neurosci. Off. J. Soc. Neurosci.* **37**, 4692–4704 (2017).
20. Fattori, V., Borghi, S. M. & Verri, W. A. Jr. IL-33/ST2 signaling boosts inflammation and pain. *Proc. Natl Acad. Sci. USA* **114**, E10034–E10035 (2017).
21. Fattori, V. et al. Targeting IL-33/ST2 signaling: regulation of immune function and analgesia. *Expert Opin. Ther. Targets* **21**, 1141–1152 (2017).
22. Li, P., Yu, Q., Nie, H., Yin, C. & Liu, B. IL-33/ST2 signaling in pain and itch: cellular and molecular mechanisms and therapeutic potentials. *Biomed. Pharmacother.* **165**, 115143 (2023).
23. Verri, W. A. et al. IL-33 mediates antigen-induced cutaneous and articular hypernociception in mice. *Proc. Natl. Acad. Sci. USA* **105**, 2723–2728 (2008).
24. Han, P. et al. Interleukin-33 mediates formalin-induced inflammatory pain in mice. *Neuroscience* **241**, 59–66 (2013).
25. Han, P. et al. Inhibition of spinal interlukin-33/ST2 Signaling and downstream ERK and JNK pathways in electroacupuncture analgesia in formalin mice. *PloS ONE* **10**, e0129576 (2015).
26. Zarpelon, A. C. et al. IL-33/ST2 signalling contributes to carrageenin-induced innate inflammation and inflammatory pain: role of cytokines, endothelin-1 and prostaglandin E2. *Br. J. Pharmacol.* **169**, 90–101 (2013).
27. Yin, C. et al. IL-33/ST2 induces neutrophil-dependent reactive oxygen species production and mediates gout pain. *Theranostics* **10**, 12189–12203 (2020).
28. He, Z. et al. Blockade of IL-33 signalling attenuates osteoarthritis. *Clin. Transl. Immunol.* **9**, e1185 (2020).
29. Huang, S. J. et al. Inhibition of spinal interleukin-33 attenuates peripheral inflammation and hyperalgesia in experimental arthritis. *Mol. Neurobiol.* **59**, 2246–2257 (2022).
30. Liu, S. et al. Spinal IL-33/ST2 signaling contributes to neuropathic pain via neuronal CaMKII–CREB and astroglial JAK2–STAT3 cascades in mice. *Anesthesiology* **123**, 1154–1169 (2015).
31. Zarpelon, A. C. et al. Spinal cord oligodendrocyte-derived alarmin IL-33 mediates neuropathic pain. *FASEB J. Off. Publ. Fed. Am. Soc. Exp. Biol.* **30**, 54–65 (2016).
32. Zeng, Y. et al. Reduction of silent information regulator 1 activates interleukin-33/st2 signaling and contributes to neuropathic pain induced by spared nerve injury in rats. *Front. Mol. Neurosci.* **13**, 17 (2020).
33. Kimura, Y. et al. IL-33 induces orofacial neuropathic pain through Fyn-dependent phosphorylation of GluN2B in the trigeminal spinal subnucleus caudalis. *Brain Behav. Immun.* **99**, 266–280 (2022).
34. Huang, J. et al. Hyperactivity of innate immunity triggers pain via TLR2-IL-33-mediated neuroimmune crosstalk. *Cell Rep.* **33**, 108233 (2020).
35. Huang, J., Gadotti, V. M., Zhang, Z. & Zamponi, G. W. The IL33 receptor ST2 contributes to mechanical hypersensitivity in mice with neuropathic pain. *Mol. Brain* **14**, 35 (2021).
36. Shi, C. & Pamer, E. G. Monocyte recruitment during infection and inflammation. *Nat. Rev. Immunol.* **11**, 762–774 (2011).
37. Tanaka, T., Minami, M., Nakagawa, T. & Satoh, M. Enhanced production of monocyte chemoattractant protein-1 in the dorsal root ganglia in a rat model of neuropathic pain: possible involvement in the development of neuropathic pain. *Neurosci. Res.* **48**, 463–469 (2004).
38. Kao, D.-J. et al. CC chemokine ligand 2 upregulates the current density and expression of TRPV1 channels and Nav1.8 sodium channels in dorsal root ganglion neurons. *J. Neuroinflamm.* **9**, 189 (2012).
39. Belkouch, M. et al. The chemokine CCL2 increases Nav1.8 sodium channel activity in primary sensory neurons through a Gβγ-dependent mechanism. *J. Neurosci. Off. J. Soc. Neurosci.* **31**, 18381–18390 (2011).
40. Xie, R. G. et al. Spinal CCL2 promotes central sensitization, long-term potentiation, and inflammatory pain via CCR2: further insights into molecular, synaptic, and cellular mechanisms. *Neurosci. Bull.* **34**, 13–21 (2018).
41. Wu, X. B., Zhu, Q. & Gao, Y. J. CCL2/CCR2 contributes to the altered excitatory-inhibitory synaptic balance in the nucleus accumbens shell following peripheral nerve injury-induced neuropathic pain. *Neurosci. Bull.* **37**, 921–933 (2021).
42. Zhang, H. et al. Spinal CCL2 promotes pain sensitization by rapid enhancement of NMDA-induced currents through the ERK-GluN2B pathway in mouse lamina II neurons. *Neurosci. Bull.* **36**, 1344–1354 (2020).
43. Liu, Y., Beyer, A. & Aebersold, R. On the dependency of cellular protein levels on mRNA abundance. *Cell* **165**, 535–550 (2016).
44. Gao, T.-C., Wang, C.-H., Wang, Y.-Q. & Mi, W.-L. IL-33/ST2 Signaling in the pathogenesis of chronic pain and itch. *Neuroscience* **529**, 16–22 (2023).
45. Raghu, H. et al. CCL2/CCR2, but not CCL5/CCR5, mediates monocyte recruitment, inflammation and cartilage destruction in osteoarthritis. *Ann. Rheum. Dis.* **76**, 914–922 (2017).
46. Liu, Z., Murphy, S. F., Wong, L., Schaeffer, A. J. & Thumbikat, P. Neuronal/astrocytic expression of chemokine (C-C motif) ligand 2 is associated with monocyte/macrophage recruitment in male chronic pelvic pain. *Pain* **161**, 2581–2591 (2020).
47. Zhang, L. et al. Key role of CCR2-expressing macrophages in a mouse model of low back pain and radiculopathy. *Brain Behav. Immun.* **91**, 556–567 (2021).
48. Van Steenwinckel, J. et al. Stromal cell-derived CCL2 drives neuropathic pain states through myeloid cell infiltration in injured nerve. *Brain. Behav. Immun.* **45**, 198–210 (2015).

49. Bawazeer, M. A. & Theoharides, T. C. IL-33 stimulates human mast cell release of CCL5 and CCL2 via MAPK and NF-κB, inhibited by methoxyluteolin. *Eur. J. Pharmacol.* **865**, 172760 (2019).
50. Hu, W. T. et al. IL-33 enhances proliferation and invasiveness of decidual stromal cells by up-regulation of CCL2/CCR2 via NF-kappaB and ERK1/2 signaling. *Mol. Hum. Reprod.* **20**, 358–372 (2014).
51. Klein Wolterink, R. G. J., Wu, G. S., Chiu, I. M. & Veiga-Fernandes, H. Neuroimmune interactions in peripheral organs. *Annu. Rev. Neurosci.* **45**, 339–360 (2022).
52. Han, S. B. et al. Transient receptor potential vanilloid-1 in epidermal keratinocytes may contribute to acute pain in herpes zoster. *Acta Derm. Venereol.* **96**, 319–322 (2016).
53. Du, L. et al. Transient receptor potential melastatin 8 contributes to the interleukin-33-mediated cold allodynia in a mouse model of neuropathic pain. *Pain* **166**, 347–359 (2024).
54. Jung, H., Toth, P. T., White, F. A. & Miller, R. J. Monocyte chemoattractant protein-1 functions as a neuromodulator in dorsal root ganglia neurons. *J. Neurochem.* **104**, 254–263 (2008).
55. Spicarova, D., Adamek, P., Kalynovska, N., Mrozkova, P. & Palecek, J. TRPV1 receptor inhibition decreases CCL2-induced hyperalgesia. *Neuropharmacology* **81**, 75–84 (2014).
56. Huang, J. et al. A neuronal circuit for activating descending modulation of neuropathic pain. *Nat. Neurosci.* **22**, 1659–1668 (2019).
57. Brenner, D. S., Golden, J. P. & Gereau, R. W. t. A novel behavioral assay for measuring cold sensation in mice. *PloS ONE* **7**, e39765 (2012).
58. Liu, X. G. & Sandkühler, J. The effects of extrasynaptic substance P on nociceptive neurons in laminae I and II in rat lumbar spinal dorsal horn. *Neuroscience* **68**, 1207–1218 (1995).
59. Zhou, L. J. et al. Microglia are indispensable for synaptic plasticity in the spinal dorsal horn and chronic pain. *Cell Rep.* **27**, 3844–3859.e3846 (2019).

Acknowledgements

This work was supported by grants from Natural Science Foundation of Guangdong Province (2023A1515012226 to J.H., and 2021A1515011516 to T.L.), the National Natural Science Foundation of China (82171211 to J.H.), the Fundamental Research Funds for the Central Universities, Sun Yat-sen University (23qnpy130 to J.H.), the Guangdong Project (2021QN02Y078 to J.H.), Science and Technology Planning Project of Guangzhou (No. 202102080239 to T.L.), Guangdong Basic and Applied Basic Research Foundation (2022B1515120026 to J.X.).

Author contributions

Junting Huang and Linjie Wang conceived the project and designed experiments. Linjie Wang, Jingyun Zhang, Shijuan Qiu, Ruizhen Huang, Yuge Wang, Yuting Wang, Mingyu Li and Qingqing Ye performed qPCR, pain behavioral tests, immunostaining, imaging, cell experiments, drug treatment and ELISA, analyzed data and co-wrote the manuscript. Ruizhen Huang performed LTP experiments, analyzed data and co-wrote the manuscript. Sibo Zhang and Zhenhua Qi helped for the behavioral experiments, tissue collection and immunostaining. Guohao Li and Denghui Xie helped for the clinical sample collection, Wenli Mi generated mouse lines. Junting Huang, Jingdun Xie, Tao Luo and Huaqiao Wang supervised the study and co-wrote the manuscript.

Competing interests

The authors declare no competing interests.

Additional information

Supplementary information The online version contains supplementary material available at https://doi.org/10.1038/s42003-025-08119-3.

Correspondence and requests for materials should be addressed to Junting Huang.

Peer review information *Communications Biology* thanks the anonymous reviewers for their contribution to the peer review of this work. Primary Handling Editors: Connie Wong and Mengtan Xing. A peer review file is available.